CQD ICDD Poster Draws a Crowd; will be on long-term display

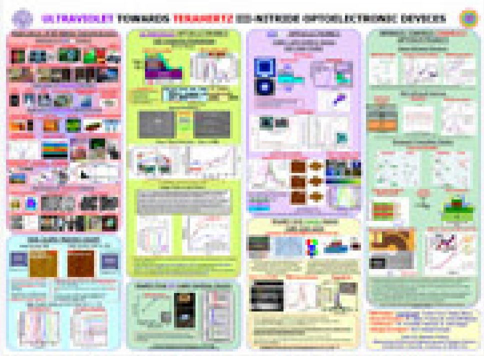

Center for Quantum Devices Poster for ICDD 2011

The Center for Quantum Devices (CQD) team designed a poster for the 2011 International Centre for Diffraction Data (ICDD) Spring Meeting, held March 14-18, 2011 in Newton Square, PA. The poster, entitled "Ultraviolet Towards Terahertz III-Nitrode Optoelectronic Devices," was such a success that the ICDD president requested the poster be kept on display throughout the year. The team consists of PhD students **Can Bayram**, **Erdem Cicek**, and **Yinjun Zhang**; Research Scientists Dr. **Zahra Vashasi** and Dr. **Ryan McClintock**; Collaborators Dr. **Ferechteh Teherani**, Dr. **Dave Rogers**, and Principal Investigator Prof. **Manijeh Razeghi**.

[click to view the poster]

SIGE by Kubik-Rubik.de

ULTRAVIOLET TOWARDS TERAHERTZ III-NITRIDE OPTOELECTRONIC DEVICES

Applications of III-Nitride Optoelectronics

Applications of Visible Emitters

Blue, Green, White Lighting Source | Automotive Lighting | Back-lighting | Displays | Mobile Technologies

Household Lighting | Interior/Exterior Illumination | Architectural Lighting

Applications of Ultraviolet Emitters

White Lighting | Water Purification | Laser Printing | Food Sterilization | High Density Optical Data Storage | In-situ activation of drugs through optical stimulus

Applications of Ultraviolet Photodetectors

Flame Detection and Combustion Monitoring | Power Line Monitoring (λ < 280 nm) | Astronomy | Non-Line-of-Sight Communication

Calibration of Light Sources in UV Therapy | Vitamin D Synthesis | Chemical and Biological Agent Detection

Terrestrial & Aerial Countermeasures | Early Missile Threat Warning | Covert Space Communications

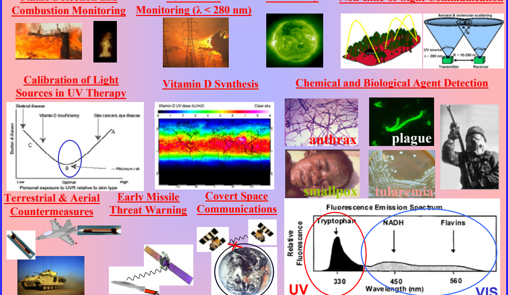

Applications of Terahertz Emitters

Dental Caries Detection | Biomedical Imaging | Cancer Detection

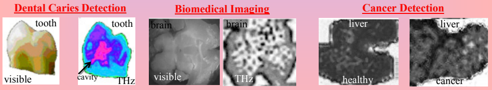

Explosives Detection | Concealed Weapons Detection | Drug Detection | Astronomy

High Quality Material Growth

High-Quality AlN

High-Quality GaN on AlN

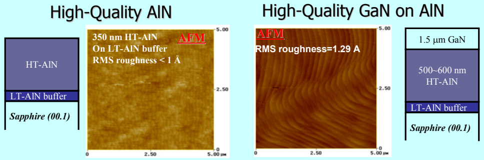

- AFM shows well ordered atomic steps, with an RMS Roughness of <1 Å for a 5µm square.
- Open Detector X-ray diffraction shows symmetric (002) and asymmetric (105) FWHMs of 41" and 240" respectively

- AFM shows well ordered atomic steps, with an RMS Roughness of ~1.29 Å for a 5µm square.
- Open Detector X-ray diffraction shows symmetric (002) FWHMs of 82".
- PL shows a narrow emission at 361 nm, FWHM~40 meV.
- Hall measurements yield a mobility of 450~500 cm²/V·s for n~10¹⁶ cm⁻³ in undoped GaN.

High Quality $Al_xGa_{1-x}N$ Thin Films ($0 \le x \le 1$)

Photoluminescence

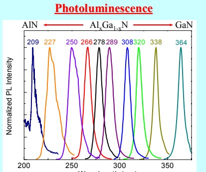

UV Optical Transmission

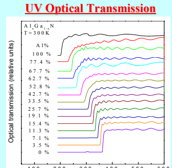

ULTRAVIOLET OPTOELECTRONICS

GaN Avalanche Photodiodes

Device Design

Device Cross-section

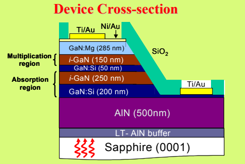

Electric field profile

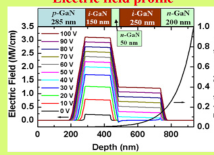

Back-Illuminated

- Back illumination is necessary for the realization of hybridizable arrays.
- Specifically designed for hole-initiated multiplication.

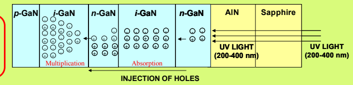

Device Processing

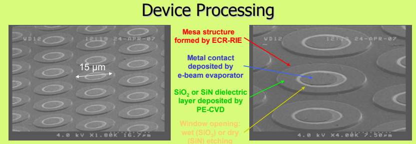

Linear Mode Operation - Gain of APD

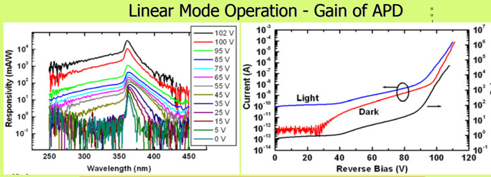

Near **53000 gain** is achieved above breakdown voltage.

Geiger Mode Single Photon

Geiger mode: Operation of avalanche photodiodes above the breakdown voltage in combination with avalanche quenching circuitry, which enables the detection of single photons. The electric field is sufficiently high that a single charge carrier injected into the multiplication layer can trigger a self-sustained avalanche. The current rises swiftly (nanosecond or subnanosecond rise time) to a macroscopic steady level in the milliampere range. If the primary carrier is photogenerated, the leading edge of the avalanche pulse marks the arrival of the detected photon. The current continues to flow until the avalanche is quenched by the circuitry, by lowering the bias voltage to below the breakdown voltage. The bias voltage is then restored in order to be able to detect another photon.

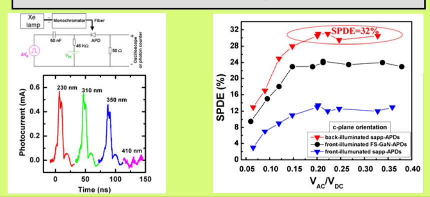

- The pulse detection efficiency was measured at different photon fluxes (photons/pulse) by varying the incident optical power.
- At high photon fluxes, the **pulse detection efficiency is 100 %** and approaches the **single photon detection efficiency (SPDE)** value as we reduce the number of photons per pulse.
- SPDE of 12% achieved under front-illumination has been improved to **32%** under back-illumination.
- We have demonstrated **world's first solar blind single photon detectors**.

World's First UV Light Emitting Diodes

Pulsed Power of LEDs

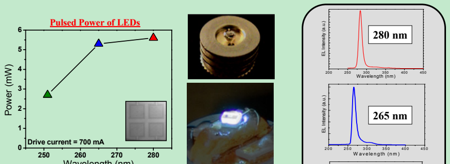

We have demonstrated the first milliwatt-level deep UV LEDs operating at 280, 265, and 250 nm, among the shortest wavelengths ever reported.

"AlGaN-based deep UV light emitting diodes with peak emission below 255 nm," Proc. SPIE 5732, 197 (2005).
"4.5 mW Operation of AlGaN-based 267 nm Deep-Ultraviolet Light-Emitting Diodes," App. Phys. Lett. 83 (2003).
"High Power 280 nm AlGaN Light Emitting Diodes Based on an Asymmetric Single Quantum Well," App. Phys. Lett. 84 (2004).

VISIBLE OPTOELECTRONICS

Visible Light Emitting Diodes and Laser Diodes

BLUE Regime

Blue & Green LEDs | Blue Laser Diode

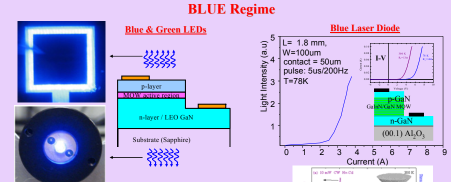

We have demonstrated blue laser diodes, high-power blue and green LEDs, and are currently pursuing green laser diodes.

Green Regime

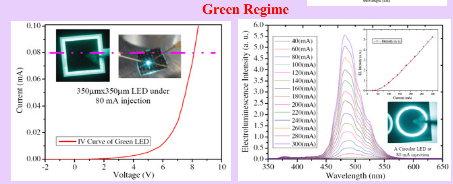

InGaN Self-Assembled Quantum Dots for Green Emitters | InGaN Tunability in the Entire Visible Regime

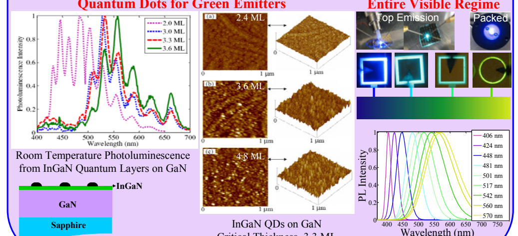

Room Temperature Photoluminescence from InGaN Quantum Layers on GaN

InGaN QDs on GaN Critical Thickness~3.3 ML

"Comprehensive study of blue and green multi-quantum-well light emitting diodes grown on conventional and lateral epitaxial overgrowth GaN," App. Phys. B (2008).

World's First Green Hybrid GaN–ZnO LEDs

Motivation: The Indium Diffusion & The Green Gap

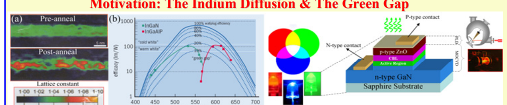

(a) HR-TEM Lattice Parameter Mapping of pre- and post-annealed InGaN active layers showing thermally-induced indium non-uniformity in InGaN, (b) The efficacy drop of the InGaN and InGaAlP LEDs in green spectra

(a) Generation of white lighting via color-mixing of red, green and blue LEDs, (b) Hybrid green LED structure, (c) The growth techniques used: MOCVD growth for GaN, InGaN active layer and AlGaInN current blocking layer, PLD growth for atop ZnO layer.

Device Cross-section | XRD Characterization | Device Results

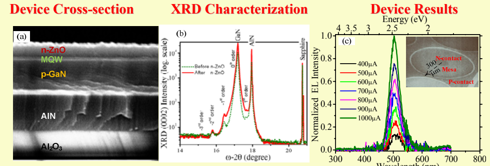

- ZnO is used as *n*-layer in (In)GaN **green** LED with inverted p-n structure ,
- High crystallographic quality of LED and integrity of MQWs are confirmed by XRD,
- Device V_{ON} = 2.5 V and green EL peaked at around 510 nm,
- **Thermal degradation of InGaN is combated through adoption of PLD for ultimate (n-ZnO) growth step (lower Ts than MOCVD of n-GaN).**
- PLD-grown ZnO may be good alternative to GaN for *n*-layer in green LEDs,
- Inversion of *p-n* junction (so that *n*-ZnO becomes top layer) also reduces total internal reflection -> improved light extraction.

"A hybrid green light-emitting diode comprised of n-ZnO/(InGaN/GaN) multi-quantum-wells/p-GaN," App. Phys. Lett., Vol. 93, 081111 (2008).
"Electroluminescence at 375 nm from a ZnO/GaN:Mg/c-Al_2O_3 heterojunction light emitting diode," App. Phys. Lett., Vol. 88, 14 (2006).

INFRARED TOWARDS TERAHERTZ OPTOELECTRONICS

Near-Infrared Devices

MOCVD Growth | Material Characterization | ISB Measurements

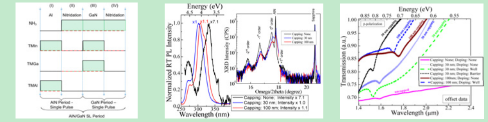

"Pulsed Metalorganic Chemical Vapor Deposition of High Quality AlN/GaN Superlattices for Near-Infrared Intersubband Transitions," App. Phys. Lett. 94, 121902 (2009).
"Effects of well width and growth temperature on optical and structural characteristics of AlN/GaN superlattices grown by metal-organic chemical vapor deposition," App. Phys. Lett. 95, 201906 (2009).

Mid-Infrared Devices

Superlattice Structure | Simulation | ISB Measurements

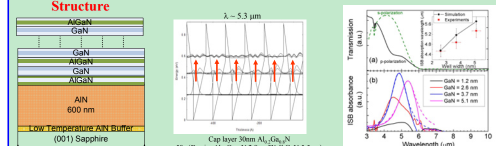

Cap layer 30nm $Al_{0.2}Ga_{0.8}N$
50×{Barrier $Al_{0.2}Ga_{0.8}N$ 2.8nm/Well GaN 5.5nm}

"Tunability of Intersubband absorption from 4.5 to 5.3 µm in a GaN/Al0.2Ga0.8N superlattices grown by metalorganic chemical vapor deposition," App. Phys. Lett. 95, 131109 (2009).

Resonant Tunneling Diodes

Operational Principles

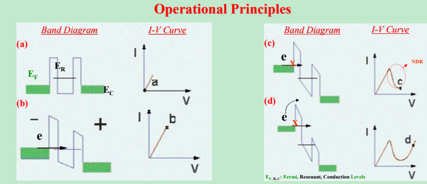

Active Layer Design & Band Structure | Crystal Directions | Device Structure

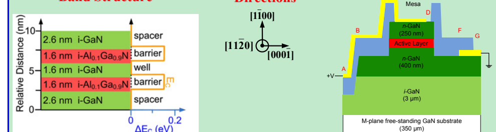

Optical micrograph / SEM of RTDs | RTD IV Curves (at 300 K and 77K)

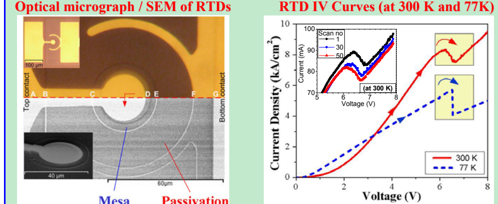

- As active layer has been identified as the main bottleneck in NDR reproducibility, nonpolar free-standing substrates employing even lower aluminum content (10%) barrier are employed.
- $Al_{0.1}Ga_{0.9}N$/GaN-based RTD devices were processed into 35-µm-diameter devices with a bridge structure on m-plane freestanding substrates.
- For the first time, a reliable and reproducible negative differential resistance at room temperature (R of - 67 Ω and current-peak-to-valley ratio of 1.08) in III-nitride RTDs was demonstrated.
- The NDR was reproducible for more than 50 scans at room temperature.

Reliability in room-temperature negative differential resistance characteristics of low-aluminum-content AlGaN/GaN double-barrier resonant tunneling diodes," App. Phys. Lett. 97, 181109 (2010).

PhD Students: Can Bayram*, Erdem Cicek, Yinjun Zhang
Research Scientists: Dr. Zahra Vashaei, Dr. Ryan McClintock
Collaborators: Dr. Ferechteh Teherani, Dr. Dave Rogers
Principal Investigator: Prof. Manijeh Razeghi

Center for Quantum Devices,
Department of Electrical Engineering and Computer Science,
Northwestern University, Evanston, IL 60208, USA